25th ABCM International Congress of Mechanical Engineering
October 20-25, 2019, Uberlândia, MG, Brazil

COB-2019-0965
THE INFLUENCE OF SMALL DEFECTS ON THE FATIGUE LIMIT OF 1045 STEEL

Daniel Moreira Oliveira
Departamento de Engenharia Mecânica, Universidade de Brasília – UnB, Brasília, DF, Brasil.
danieljedail@hotmail.com

Artur Lopes Dias
Cainã Bemfica de Barros
Roberto Azevedo da Costa
Fábio Comes de Castro
Departamento de Engenharia Mecânica, Universidade de Brasília – UnB, Brasília, DF, Brasil.
artur.dias@ifb.edu.br, cainabemfica@gmail.com, robertoac.enm@gmail.com, fabiocastro@unb.br

Abstract. *This work investigates the influence of small surface defects on the fatigue limit of SAE 1045 steel. Uniaxial fatigue tests were performed on solid specimens with a cylindrical defect of* $\sqrt{area}$ *= 400 μm at load ratios R = -1 and 0.1. Fatigue cracks were observed to initiate close to the point of maximum principal stress at the hole edge and to propagate approximately in the plane perpendicular to the direction of the maximum principal stress. The Walker relationship was extended to include the effect of small defects on the fatigue limit, giving estimates as good as the ones from the Murakami–Endo relationship.*

Keywords: *1045 steel, small defect, fatigue limit,* $\sqrt{area}$.

1. INTRODUCTION

Small surface defects such as scratches and flaws are often present in many engineering components. They may arise from the manufacturing process or handling operations, or from environmental action (e.g., corrosion pits). Experimental evidences have clearly indicated the deleterious influence of small defects on the fatigue strength of materials (Murakami, 2002). Hence, their effects should be properly understood to guarantee the safety of components subjected to cyclic loading.

Murakami and Endo have developed a fracture mechanics-based approach for estimating the effect of small defects on the fatigue limit (Murakami and Nemat-Nasser, 1983; Murakami and Endo, 1983; Murakami and Endo, 1986; Murakami, 2012). The main assumption of the Murakami–Endo approach is that the square root of the area obtained by projecting the defect onto the plane perpendicular to the maximum tensile stress, $\sqrt{\text{area}}$, is the appropriate geometrical parameter to be used when estimating the effect of a defect on the fatigue strength.

The formula developed by Murakami and Endo for estimating the fatigue limit of a material containing a surface defect is

$$\sigma_{\text{w}} = \frac{1.43(H_{\text{v}} + 120)}{\left(\sqrt{\text{area}}\right)^{1/6}}\left[\frac{1-R}{2}\right]^{\alpha} \tag{1}$$

where σ_{w} is the fatigue limit, H_{v} is the Vickers hardness, R is the ratio of the minimum stress over the maximum stress in a loading cycle, and α is a mean stress sensitivity factor calculated as $\alpha = 0.226 + H_{\text{v}} \times 10^{-4}$.

The purpose of the present study is to investigate the effect of a small cylindrical defect on the fatigue limit of SAE 1045 steel at two stress ratios (R = -1 and 0.1). This steel is often chosen by engineers of the ground vehicle industry for manufacturing structural components subjected to cyclic loading, such as crankshafts and conrods.

2. MATERIAL AND EXPERIMENTS

The SAE 1045 steel was received as drawn cylindrical bars of 19.05 mm diameter. The chemical composition of the material in weight percentage is 0.46% C, 0.66% Mn, 0.19% Si, 0.012% S, 0.022% P, and Fe as balance. Bars were annealed at 845 ºC to relieve residual stresses due to the drawing process. The resulting microstructure, which consists of

ferrite and pearlite, is shown in Fig. 1. The monotonic properties of the annealed SAE 1045 are listed in Table 1. The Vickers hardness after annealing was H_v = 199, which is a mean value of measurements at three points with a load of 30 kgf. The scatter of *HV* is within 3%.

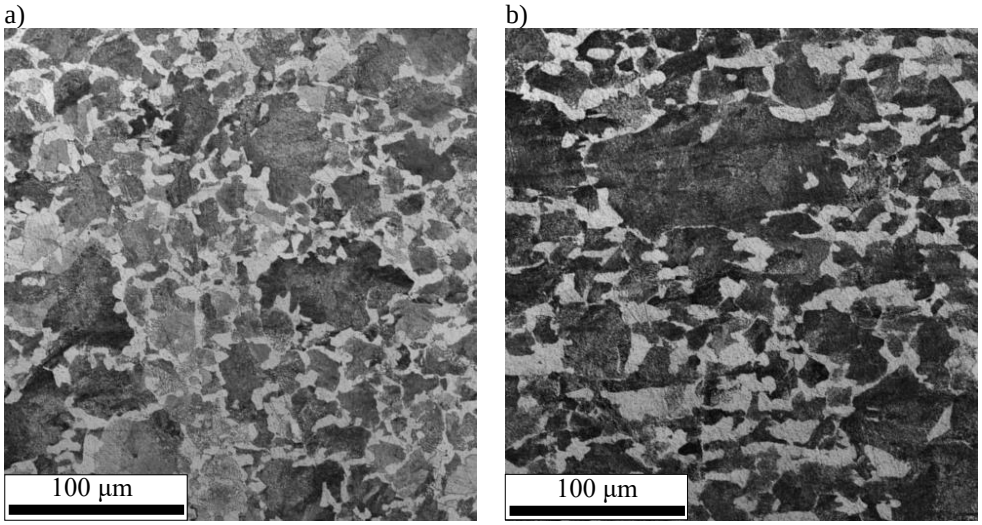

Figure 1. Microstructure of the annealed SAE 1045 steel: (a) transverse and (b) longitudinal sections.

Table 1. Mechanical properties of the annealed SAE 1045 steel.

0.2%-offset yield stress	Ultimate tensile strength	Young's modulus	Vickers Hardness
326 MPa	661 MPa	216 GPa	199 HV

After annealing, solid specimens with the geometry shown in Fig. 2a were machined and ground with sandpapers whose grit numbers ranged from 220 to 2500. Afterwards, a small cylindrical defect of $\sqrt{area}$ = 400 µm was drilled at the center of the gage section (Fig. 2b). Dimensional measurements made with an Olympus LEXT OLS 4100 confocal microscope revealed that the variation of the defect size, $\sqrt{area}$, from the target value of 400 µm was within 5%.

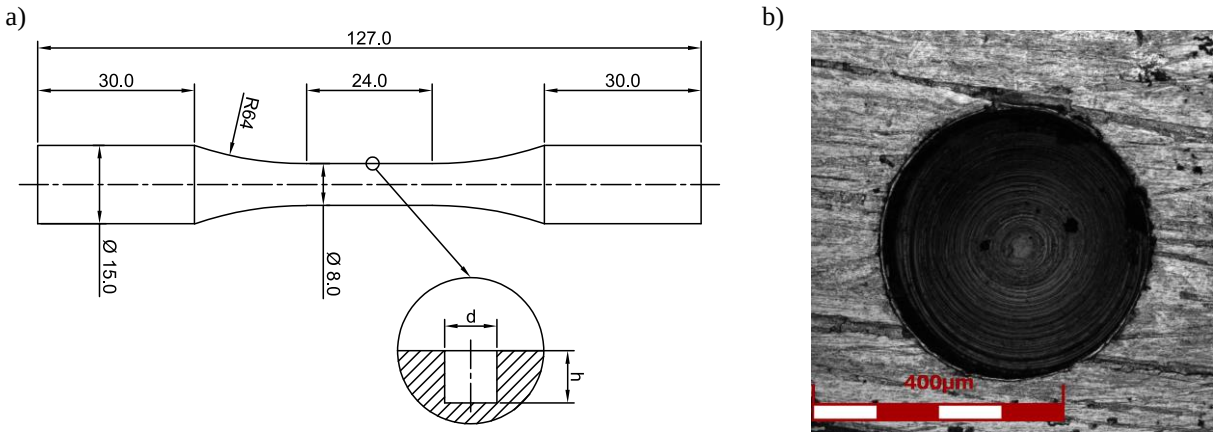

Figure 2. (a) Specimen and defect geometry (dimensions in mm); (b) micrograph of the drilled defect.

Fully reversed force-controlled fatigue tests were conducted on an MTS servo-hydraulic testing system with loading frequencies ranging from 20 to 45 Hz. The experimental results are summarized in Table 2. The tests were carried out until total fracture of the specimen into two parts or until 10^7 cycles (run-out specimen). The fatigue limit was defined as the greatest stress amplitude at which run out occurred.

Table 2. Results of uniaxial fatigue tests.

$\Delta\sigma/2$ (MPa)	R	N_f (cycles)	Note
220	-1	86,791	Failure from defect
200	-1	451,634	Failure from defect
180	-1	5,703,237	Failure from defect
160	-1	–	Run-out at $N = 10^7$ cycles
150	0.1	670,259	Failure from defect
130	0.1	–	Run-out at $N = 10^7$ cycles

3. RESULTS AND DISCUSSION

Fatigue cracks were consistently observed to initiate at the point of maximum principal stress at the hole surface. They propagated approximately in the plane perpendicular to the direction of the maximum principal stress. Figure 3 shows the fatigue crack observed after 10^7 cycles (run out) in the specimen subjected to fully reversed loading at $\Delta\sigma/2$ = 160 MPa. Two fatigue cracks initiated close to the point of maximum principal stress at the hole edge. Crack lengths were 136 µm and 175 µm for the left and right cracks, respectively. For the test performed at $\Delta\sigma/2$ = 130 MPa and R = 0.1, no crack was observed after 10^7 cycles.

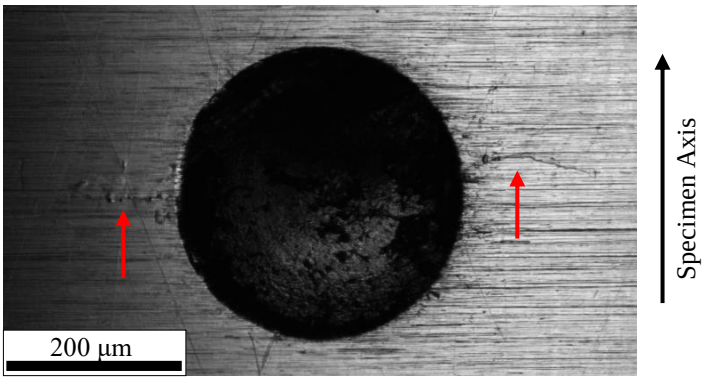

Figure 3. Fatigue cracks observed after 10^7 cycles for the fully reversed test at $\Delta\sigma/2$ = 160 MPa.

Figure 4 shows the test data for stress ratios R = -1 and 0.1 and the fatigue limit estimation given by the Murakami–Endo formula, Eq. (1). Solid symbols represent failed specimens and open symbols denote run-out specimens. The predicted fatigue limit at R = -1 is 168 MPa, which is 5% greater than the experimental value. For R = 0.1 the predicted fatigue limit is 138 MPa, which is 6% greater than the experimental value. This degree of accuracy is consistent with the results reported in Murakami (2002) for maraging and low carbon steels, for which the difference between predicted and experimental values is within ±15%.

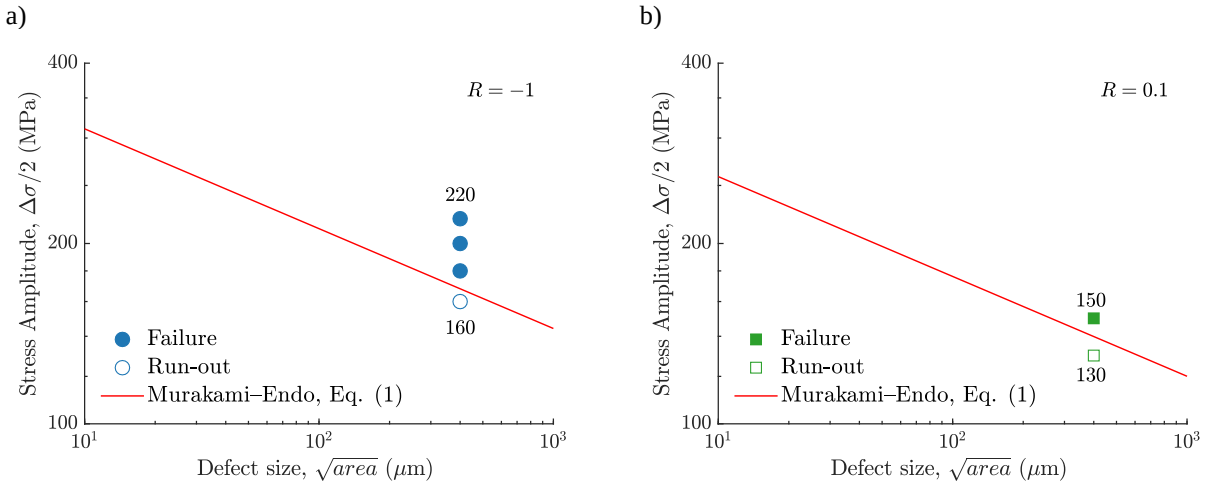

Figure 4. Stress amplitude vs. defect size for (a) R = -1 and (b) R = 0.1.

The Walker relationship (Walker, 1970; Dowling et al., 2009) is now extended to include the effect of small defects on the fatigue limit as follows:

$$\sigma_{\mathrm{a}}^{m}\sigma_{\max}^{1-m} = \frac{1.43(H_{\mathrm{v}}+120)}{\left(\sqrt{\mathrm{area}}\right)^{1/6}} \tag{2}$$

In Eq. (2), the left-hand side can be thought of as an *equivalent fully reversed stress amplitude*, while the right-hand side is the fatigue limit of the material for a defect size of $\sqrt{\mathrm{area}}$ and fully reversed axial loading (R = -1). The quantity $1-m$ can be regarded as a mean stress sensitivity factor. If m = 0.5, Eq. (2) reduces to the Smith–Watson–Topper relationship. The advantage of the Walker relationship over the Murakami–Endo formula, Eq. (1), is that it can, in principle, be applied for multiaxial stress conditions using the critical plane concept. To verify this hypothesis, multiaxial fatigue experiments on small surface defects are still needed.

An expression for m can be obtained by best fitting a representative set of fatigue limit data involving small defects. This procedure was performed by best fitting the experimental data reported by Murakami (2002) for a maraging steel (H_{v} = 740), which resulted in m = 0.55, and for a 0.13% C steel which yielded m = 0.77. Considering these values of m and H_{v}, the following linear relation can be derived:

$$m = 0.806 - 3.465\times10^{-4}\,H_{\mathrm{v}} \tag{3}$$

Figure 5 shows how the mean stress effect on the fatigue limit is described by the Murakami–Endo and the modified Walker relationships. For the SAE 1045 steel, H_{v} = 199. Thus, Eq. (3) yields m = 0.737. The accuracies of the fatigue limit estimates given by the Murakami–Endo and the modified Walker relationships are quite similar, both in very good agreement with the experimental results. A less desirable fatigue limit estimate was obtained by the Smith–Watson–Topper relationship.

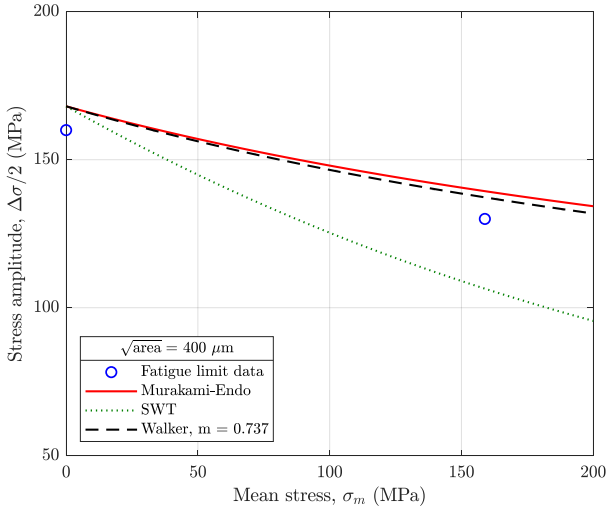

Figure 5. Comparison between fatigue limit data for SAE 1045 steel with a defect of $\sqrt{\mathrm{area}}$ = 400 μm and predictions using the Murakami–Endo and Walker relationships.

4. CONCLUSIONS

Uniaxial fatigue tests on SAE 1045 steel with a small surface defect of $\sqrt{\mathrm{area}}$ = 400 μm were conducted at stress ratios R = -1 and 0.1, which showed that fatigue cracks initiated at the point of maximum principal stress at the hole surface and propagated approximately in the plane perpendicular to the direction of the maximum principal stress. The Walker relationship was extended to include the effect of small defects on the fatigue limit, giving estimates as good as the ones from the Murakami–Endo relationship. Experiments involving more complicated defect geometries and loading histories are required to further evaluate the modified Walker relationship.

5. ACKNOWLEDGEMENTS

Daniel Moreira Oliveira is grateful to the company Hidráulica Brasil for allowing him to conduct the present study. Artur Lopes Dias would like to thank the support from Instituto Federal de Brasília – IFB. Fábio Castro would like to thank the support from National Council for Scientific and Technological Development – CNPq (308126/2016-5 and 420677/2018-6) and the support from FAP-DF (0193.001583/2017). Cainã Bemfica would like to thank the support from Coordination for the Improvement of Higher Education Personnel – CAPES.

6. REFERENCES

Dowling, N.E., Calhoun, C.A. and Arcari, A., 2002. "Mean stress effects in stress-life fatigue and the Walker equation". *Fatigue & Fracture of Engineering Materials & Structures*, Vol. 32, pp. 163–179.

Murakami, Y., 2002. *Metal Fatigue: Effects of Small Defects and Nonmetallic Inclusions*. Elsevier, Oxford, 1st edition.

Murakami, Y., 2012. "Material defects as the basis of fatigue design". *International Journal of Fatigue*, Vol. 41, No 1, pp. 2–10.

Murakami, Y. and Endo, M., 1983. "Quantitative evaluation of fatigue strength of metals containing various small defects or cracks". *Engineering Fracture Mechanics*, Vol. 17, No. 1, pp. 1–15.

Murakami, Y. and Endo, M., 1986. "Effects of hardness and crack geometries on ΔK_{th} of small cracks emanating from small defects". *K.J. Miller, E.R. de Los Rios (Eds.), The Behavior of Short Fatigue Crack, Mechanical Engineering Publications*, Vol. 1, No. 1, pp. 275–293.

Murakami, Y. and Nemat-Nasser, S., 1983. "Growth and stability of interacting surface flaws of arbitrary shape". *Engineering Fracture Mechanics*, Vol. 17, No. 3, pp. 193–210.

Walker, K., 1970. "The effect of stress ratio during crack propagation and fatigue for 2024-T3 and 7075-T6 aluminum". Effects of Environment and Complex Load History on Fatigue Life. ASTM STP 462, Am. Soc. for Testing and Materials, Philadelphia, PA, pp. 1–14.

7. RESPONSIBILITY NOTICE

The authors are the only responsible for the printed material included in this paper.